A Single-DNA Molecule Nanomotor Regulated by Photons

*Huaizhi Kang†, Haipeng Liu†, Joseph A. Phillips†, Zehui Cao†, Youngmi Kim†, Yan Chen†, Zunyi Yang‖ and Weihong Tan†**

† Department of Chemistry and Department of Physiology and Functional Genomics, Shands Cancer Center and UF Genetics Institute, Center for Research at the Bio/Nano Interface, McKnight Brain Institute, University of Florida, Gainesville, Florida 32611-7200

‖Foundation for Applied Molecular Evolution, 1115 NW 4th Street, Gainesville, FL 32601
E-mail: tan@ chem.ufl.edu.

Phone and fax: (+1) 352-846-2410

Supporting information

a. Buffer optimization

The buffer solution condition was optimized based on PSMM3 photoresponse under UV/Vis irradiation. Generally, a strong ion-strength buffer solution is able to stabilize the duplex structure (close state); it will also hinder the reverse process of destabilizing the duplex structure (open state). Therefore, proper ion strength is needed to balance this close-open conversion by setting up conditions that favor both states equally. Salt concentration was used to adjust the ion strength. High salt concentration aids base paring and improves the hybridization rate and stability of duplex (open to close), but it induces a uni-directional nanomotor with poor balance or reversible operation. On the other hand, a very low salt concentration of buffer solution will not be able to initiate a large amount of fully closed MB structure, although it does facilitate conversion between close and open states. Additionally, low salt concentration impedes the conversion rate kinetically. Therefore, we used a conventional MB buffer solution with main components of Tris-HCl (pH 8.0), NaCl and $MgCl_2$. We screened the concentration of Na^+ and Mg^{2+} from 1mM to 500 mM, and Tris-HCl concentration from 2 mM to 200 mM, as a function of photoresponse of MB duplex with UV/Vis irradiation. The optimized buffer includes the following: 20 mM Tris-HCl (pH 8.0), 20 mM NaCl, and 2 mM $MgCl_2$. Under these conditions, PSMM3 nanomotor operation displayed a well-balanced rate of open and close states.

b. Light sources optimization

In order to examine the sensitivity of azobenzene isomerization to hairpin structure upon irradiation, two groups of light sources were selected. For both groups, a 60W table lamp with a 450 nm filter had enough power to trigger fast *cis*- to *trans*- conversion and was therefore chosen as the visible light source. A Fluorolog-Tau-3 Spectrofluorometer was chosen for group one as the UV light source, and a portable 6W UV light source (both irradiate at 350 nm) was chosen for group two. The power of the two UV light sources had been measured by power meter for group one with 0.028 mW (±0.2) and for group two with 0.197mW (±0.3) at the irradiated sample position. A ten-round test was performed with these two groups of light sources in the previously selected buffer solution. Reversible photoregulation was carried out by repeated irradiations at 450 nm and 350 nm, followed by emission scans (λ_{ex}= 488 nm). In all cases, the low power spectrofluorometer could not initiate a fluorescence variation over 5% with up to 20 minutes of irradiation. However, the high power portable light source was observed to drive the variation up to 60%, depending on buffer solutions and irradiation time. Therefore, the portable UV lamp was selected as the UV light source for the following experiments. We believe that an even stronger UV light source will help improve the *trans*- to *cis*- conversion, even though its use raises serious problems in terms of damaging the DNA structure and photobleaching the fluorophore. Photobleaching was observed with our portable UV lamp for long-term irradiation over 30 minutes.

c. Synthesis of azobenzene phosphoramidite monomer (Azo-)

In order to obtain a photoregulated phosphoramidite monomer, azobenzene was selected for its reversible photoregulation property. D-Threoninol was chosen here as the linker for synthesizing optically pure diols. The synthesis routes are similar to published protocol and are shown as **Scheme S1**.[1] **Compound 1.** ^{1}H NMR ($CDCl_3$): δ 7.96-7.38 (m, 9H), δ 7.12 (d, 1H), δ 4.33 (m, 1H), δ 4.09 (m, 1H), δ 3.98 (d, 2H), δ 1.29 (d, 3H). **Compound 2**. ^{1}H NMR ($CDCl_3$): δ 8.00-6.78 (m, 23H), δ 4.25 (m, 1H), δ 4.17 (m, 1H), δ 3.77 (s, 6H), δ 3.60 and 3.42 (dd, 2H), 1.23 (d, 3H). **Compound 3**. ^{1}H NMR ($CDCl_3$): δ 8.00-6.79 (m, 22H), δ 6.62 (d, 1H), δ 4.48 (m, 1H), δ 4.39 (m, 1H), δ 4.21-4.10 (m, 2H), δ 3.77 (s, 6H), δ 3.57-3.34 (m, 4H), δ 2.76-2.72 (m, 2H), δ 1.30-1.25 (m, 15H). ^{31}P ($CDCL_3$): δ 149.

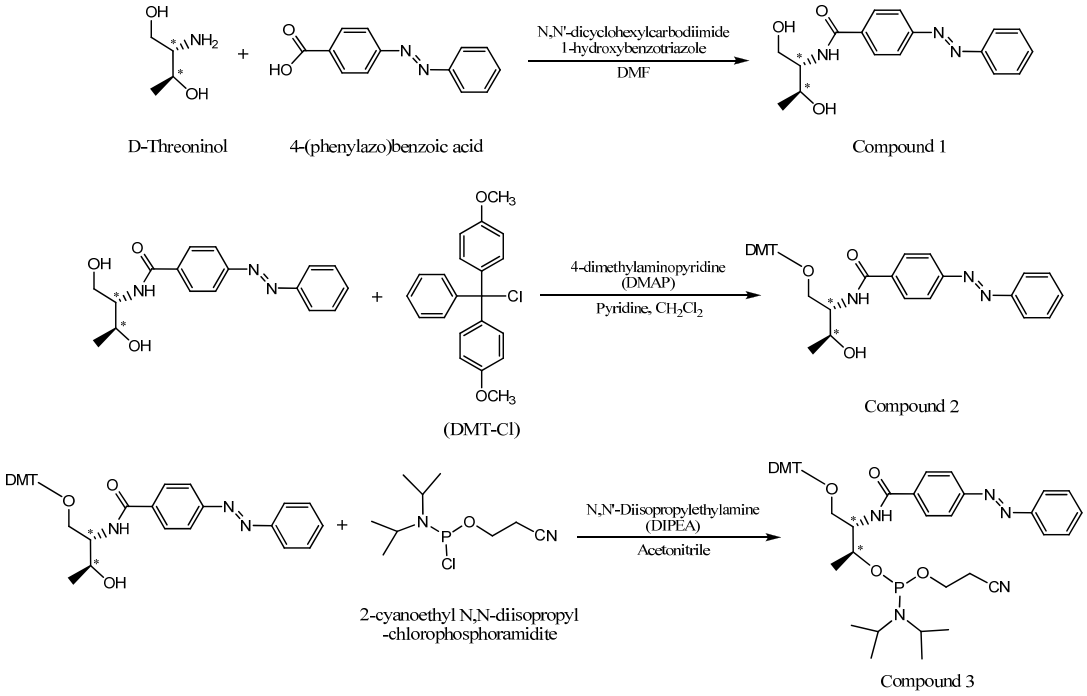

Scheme S1. Synthesis of azobenzene-tethered phosphoramidite monomer

d. Synthesis and purification of hairpin molecules

Hairpin moleclues were synthesized by using a DNA/RNA synthesizer ABI3400 (Applied Biosystems). A solid-phase synthesis method was used to couple FAM to the MBs' 5' ends. The synthesis started with a 3'-Dabcyl controlled pore glass (CPG) column at 1 μmole scale. A routine coupling program was used to couple the normal bases from 3' end on Dabcyl CPG. A proper amount of Azo- was dissolved in dry acetonitrile in a vial connected to the synthesizer (20 mg Azo- can make a single incorporation in the DNA at 1.0 μmole scale synthesis, generally Azo- coupling reagent can be prepared by dissolving in acetonitrile on 20 mg/200 μL). The coupling step can be performed in room temperature immediately after the Azo- reagent preparation.[1] It then can be regarded as a normal base for insertion in programming the synthesizer (**Scheme S2**) with at least 600 s reaction time. A coupling program of 900 s reaction time was applied to couple the 5' FAM fluorophore at the very end. After the synthesis, the CPG substrate was transferred to a glass vial, and standard AMA (ammonium hydroxide: methylamine = 1:1) deprotection solution was added and incubated in water bath at 50 °C for 12 hours. After centrifuge to separate the solid beads from MB in the solution, the clear supernatant was carefully collected. Then, the MBs were concentrated by ethanol precipitation. The precipitate was redissolved by TEAA solution (0.1 M) and delivered to reverse phase HPLC using a C18 column with a linear elution (with 30 min of gradient from 19% acetonitrile to 55%). The collected product was then vacuum dried, detritylated, and stored at -20 °C for future use.

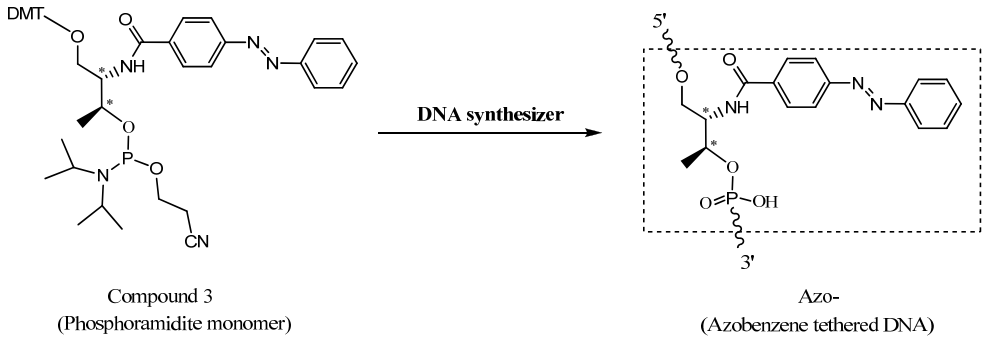

Compound 3
(Phosphoramidite monomer)

Azo-
(Azobenzene tethered DNA)

Scheme S2. Incorporation of Azo- to DNA sequences by DNA synthesizer

e. Synthesis and purification of linear sequences

The 12 bps linear sequence: 5' GGTCGCGCTAGG-Dabcyl 3', 10 bps: 5' TCGCGCTAGG-Dabcyl 3', and their cDNAs, 5' FAM-CCTAGCGCGACC 3' and 5' FAM-CCTAGCGCGA, were prepared with the same protocol by means of corresponding fluorophore and quencher coupling. For Azo- incorporated sequences, Dabcyl CPG was used for synthesis, and FAM fluorophore was labeled to cDNA. The purifications of all linear sequences followed the same protocol as MBs with reverse phase HPLC on a C18 column.

f. Characterization of PSMM

The concentration of each DNA was calculated by the absorption at 260 nm by UV spectrometer. The concentration of the unmodified PSMM can be calculated by Beer's Law according to the following formula: $c = A_{260} / d(\varepsilon_{nat})$, where c is the concentration of modified DNA (M), A_{260} is the absorbance at 260 nm, d is the thickness of the cell (cm), and ε_{nat} is the molar extinction coefficient of the native DNA. The concentration of the Azo- PSMMs can be calculated according to the following formula: $c = A_{260} / d(\varepsilon_{nat} + n\varepsilon_{azo})$, where n is the number of Azo- in the modified MBs and ε_{azo} is the extinction coefficient of the azobenzene moiety (4,100 $M^{-1}cm^{-1}$).[1]

Thermal denaturizing profiles of PSMMs and linear DNAs were measured with RT-PCR. To cover all the possible transition states, the temperature was slowly increased under the rate of 1 °C /min from 10 °C to 80 °C. The buffer solution for all the measurements is identical: 20 mM Tris buffer pH 8.0, Na^+: 20 mM, Mg^{2+}: 2 mM.

a

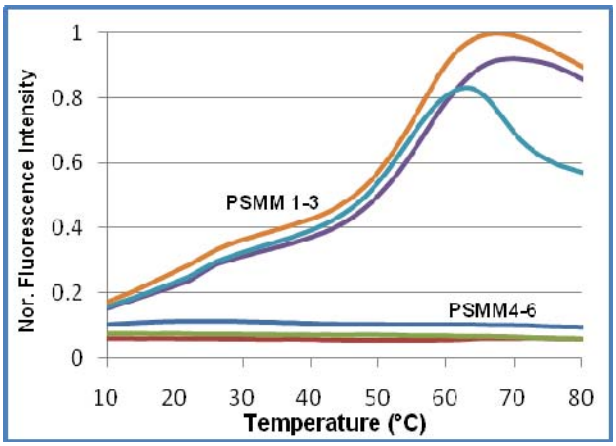

b

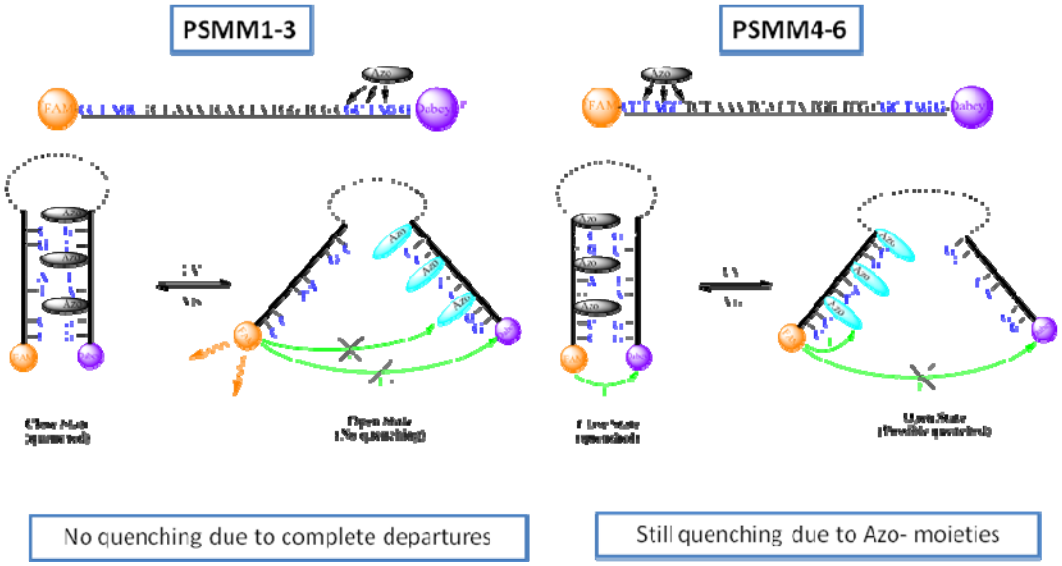

Figure S1. **a**. Melting temperature profiles of PSMM1-6 under the same conditions (The melting temperatures of PSMM1-3 were summarized in *Table S1*). The measurements were repeated twice for each sample. The concentration was 100 nM in buffer solution (buffer: 20 mM Tris buffer pH 8.0, Na^+: 20 mM, Mg^+:2 mM). **b**. Suggested mechanisms of photoresponse of PSMM1-3 (left) and PSMM4-6 (right). Pre-treatment of visible light ensured the hairpin structure formation and the lowest fluorescence background at the starting point.

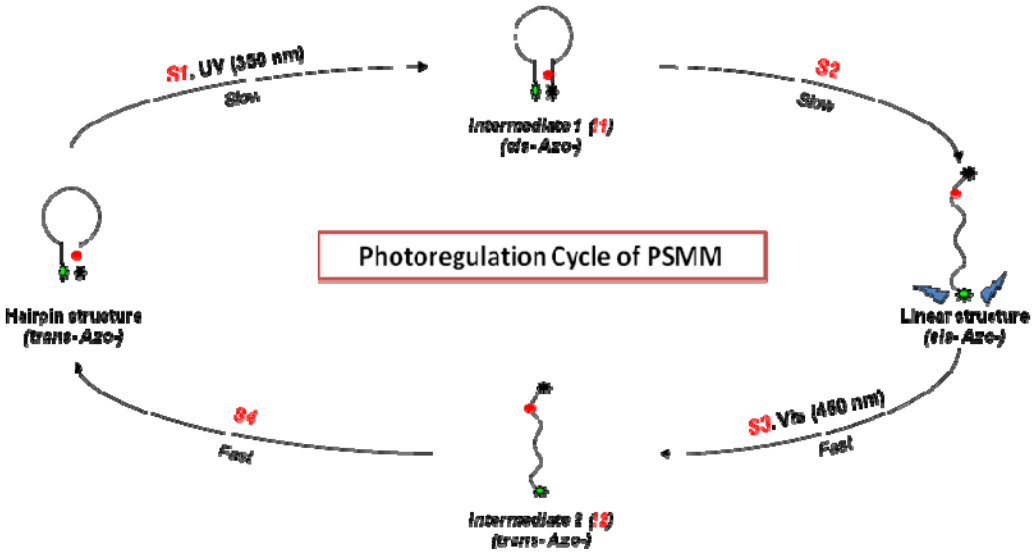

Scheme S3. A photoregulation cycle of azobenzene-incorporated hairpin nanomotor (PSMM). Under normal conditions, the azobenzene takes the stable *trans*- state, both before and after visible light irradiation, and the PSMM remains in hairpin structure. However, the *trans*- azobenzene can be converted to the unstable *cis*- state when irradiated by UV light to produce hairpin structure intermediate *1* (*S1, I1*) where the structure is about to transform with *cis*- state azobenzene destabilize the stem duplex. The *cis*- azobenzene aids in the dissociation of the stem duplex of the hairpin structure, and an extended single-strand DNA is formed (*S2*). The linear state PSMM is comparably more stable than *I1* and can stay in the dark state for minutes. Under visible light irradiation, the *cis*- azobenzene can be switched back to *trans*- state very fast (within several seconds to minutes), and a linear intermediate (*I2*) is formed (*S3*). *I2* favors a hybridization of complementary strands so that the hairpin structure reforms (*S4*). Both of the *S3* and *S4* are much faster than *S1* and *S2* due to stability of azobenzene in different conformation. The cycle is reversible by repeated UV and visible light irradiation in turn.

g. Calculation of extension and contraction forces

In order to obtain the extension and contraction forces, Gibes free energy and the distance traveled between the two ends of stem duplex were introduced for calculation. The free energies of extension and contraction processes are the same due to base paring and departing and can be calculated based on Mfold with molecular beacon hairpin structure giving ΔG = -3.56 kcal.mole^{-1}.[2] However, the forces generated by each process differ by the stiffness of the structures during each cycle. The contraction process starts from soft single-strand coil and ends with a rigid hairpin structure, illustrating that most of the free energy is converted to mechanical motion. The distance between the two arms in open state can be calculated by the length of base pairs, which is 10.2 nm. We presume that the distance in close state is the same as the dsDNA helix diameter of 2.2 nm and that the net "contraction distance" is approximately 8 nm for the 31mer. Therefore, the contraction force is 3.1 pN. The extension force is limited by the softness of single-strand structure from hairpin structure. The effective distance that the single-strand DNA can reach is determined by persistence length and can be estimated by previous study.[3] The distance is in the range of 4-5 nm. We can then derive an extension force of around 1.5 pN.

h. Open-close conversion efficiency

The ratio of opened hairpin structure *versus* the total amount of molecules is set as conversion efficiency which is represented by recovery percentage. The ratios of Azo- to bases in a molecule for different PSMMs are significantly different. Given the same length of DNA sequences, if the smaller amount of Azo- incorporation yields the same photoregulation capacity, the motor will possess a higher efficiency property under same energy input. Thus, for our 31 bases MB hairpin backbone, the maximum Azo- incorporation number is 3 in the stem,

which gives an Azo-/base ratio of 9.7% with around 50% regulation capability (the conversion efficiency is about 50%, as shown in **Figure 2**). In comparison, the reported linear DNA photoregulated nanomachines with Azo-/base ratio of 37.5% have around 60% regulation capability at elevated temperature.[4] Other reported Azo- photoregulated linear DNA probes always maintain a ratio around 45% for highly responsive photoregulation.[5-8] Therefore, we can easily conclude that photoconversion efficiency of the hairpin nanomotors is much higher than that of the linear probes. This is simply because the PSMM designed in this report is a single molecule DNA nanomotor, and intramolecular hybridization and dehybridization is much more efficient. To better quantitatively assess the two types of nanodevices, a series of linear DNAs were designed and synthesized for comparison.

In order to compare the efficiency of these DNA nanomotors as a function of sequences and length, melting temperature (T_m) was introduced as the correlated parameter to make our evaluation. Melting temperature is the temperature at which an oligonucleotide duplex is 50% in both single-stranded form and double-stranded form. A general method estimates T_m from the nearest-neighbor two-state model, which is applicable to short DNA duplexes:

$$T_m\,(^{o}C) = \Delta H^{\circ}/[\Delta S^{\circ}+R\ln C_{DNA}] - 273.15$$

where ΔH° (enthalpy) and ΔS° (entropy) are the melting parameters calculated from the sequence and the nearest-neighbor thermodynamic parameters,[32] R is the ideal gas constant (1.987 $cal\cdot K^{-1}mole^{-1}$), and C_{DNA} is the molar concentration of a DNA.

Three 12 bases linear DNAs/cDNAs bearing Azo- and Dabcyl and their cDNA-bearing FAM have been designed and synthesized (L12-1-3, L12-cDNA, Scheme S4 A). Based on M-fold calculations, experimental results show the T_ms of the L12-1, L12-2, and L12-3 linear DNAs as 55.2 ºC, 54.8 ºC and 53.7 ºC ±0.2, respectively. These values are close to those of PSMMs 1-3, with the latter value very close to PSMM3 (55.0 ºC, **Table S1**). Experimental measurements of all linear probes with their cDNA have been performed with variation within 1 ºC (data not shown).

a.

Linear sequences (12 base pairs): 53.7 °C ≤ Tm ≤ 55.2 °C
L12-cDNA: 5'FAM CCT AGC GCG ACC
L12-1: 5'GG TC GC-Azo-GC-Azo-TA-Azo-GG-Dabcyl3'
L12-2: 5'GG TC-Azo-GC-Azo-GC-Azo-TA-Azo-GG-Dabcyl3'
L12-3: 5'GG-Azo-TC-Azo-GC-Azo-GC-Azo-TA-Azo-GG-Dabcyl3'

b.

Linear sequences (10 base pairs): 47.5 °C ≤ Tm ≤ 48.6 °C
L10-cDNA: 5'(FAM) CCT AGC GCG A
L10-1: 5'TC GC-Azo-GC-Azo-TA-Azo-GG (Dabcyl)
L10-2: 5'TC-Azo-GC-Azo-GC-Azo-TA-Azo-GG (Dabcyl)

Scheme S4. The sequences of a) 12 bases Azo- incorporated linear sequences and cDNA; b) 10 bases Azo- incorporated linear sequences and cDNA

Multiple Azo- moieties have been incorporated into the L12 sequences from 3' to 5' and at the same positions as PSMM1-3, with Azo-/base of 25%, 33.3%, and 41.7%, respectively. The L12-1 has triple Azo- incorporation, which is the same as PSMM3, but with a high Azo-/base ratio (50%). Based on the comparison standard of relationship between T_m and duplex stability we set above, PSMM3 and L12-1 should have the same stability of duplex structure and should be able to absorb the same amount of photons (both have three Azo- for each molecule). If the conversion efficiency is identical for both types of Azo- molecules, we would expect the same fluorescence recovery percentage for L12-1 and PSMM3. L12-2 and L12-3 have slightly lower T_m, but since they

have more Azo- than L12-1 and PSMM3, a higher recovery is expected for these two molecules. The photoregulation properties of all L12s are displayed in **Figure S2a** under the same conditions (buffer, temperature, DNA concentration, and UV-Vis irradiation) as those being used for hairpin PSMM3. All three linear DNAs display reversible photoregulation capability with different efficiencies: 2.9% for L12-1, 5.7% for L12-2, 11.5% for L12-3. Each linear DNA was photoregulated by UV/Vis for five cycles, and each displayed reversible photoregulation for all five cycles.

The fluorescence recovery of the L12 DNA, when compared with the PSMMs, demonstrates that the PSMMs have much higher efficiency response to photon energy. Since both PSMMs and linear DNAs have the same nuclear acid unit and Azo- components, the main factor contributing to their variable efficiencies is the difference between their respective structures. Specifically, the structure of the PSMM is folded hairpin where loop moiety affects the stability of stem duplex, while linear DNAs have extended duplex structure which is only affected by strand exchange. The short stem duplex of PSMM3 with triple Azo- incorporation is highly sensitive to conformational changes of Azo- isomerization, resulting in a 54.7% change in comformation. In contrast, the linear DNAs only seem to unzip from the end incorporated with multiple Azo- with partial duplex structure so that a complete departure of their complementary DNAs is unlikely (2.9% for L12-1). Moreover, even with the saturated Azo-loading of linear DNAs (L12-3), the duplex dissociation is still very low (11.5%) at room temperature. Therefore, based on the mechanism of fluorescence variation, there are fewer linear DNA duplexes dehybridized under our experimental conditions compared to PSMM molecules. Also, the low efficiency of linear DNAs is a function of the T_ms on both *trans*- and *cis*- conformations, which are much higher than room temperature $\mathbf{T_{m(\textit{trans}\text{-})} > T_{(RT)}}$: $\mathbf{T_{m(\textit{trans}\text{-})} > T_{m(\textit{cis}\text{-})} > T_{(RT)}}$, whereas the T_ms of PSMMs, when azobenzene takes *cis*- conformations, are significantly lowered and less than room temperature: $\mathbf{T_{m(\textit{trans}\text{-})} > T_{(RT)} \geq T_{m(\textit{cis}\text{-})}}$. This result demonstrates that hairpin-based nanomotors are energy efficient motors compared with motors based on linear DNAs.

a

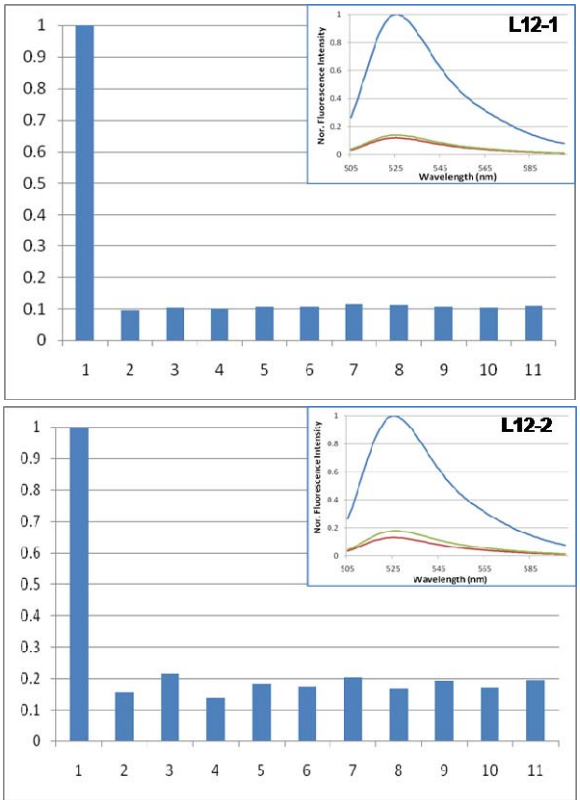

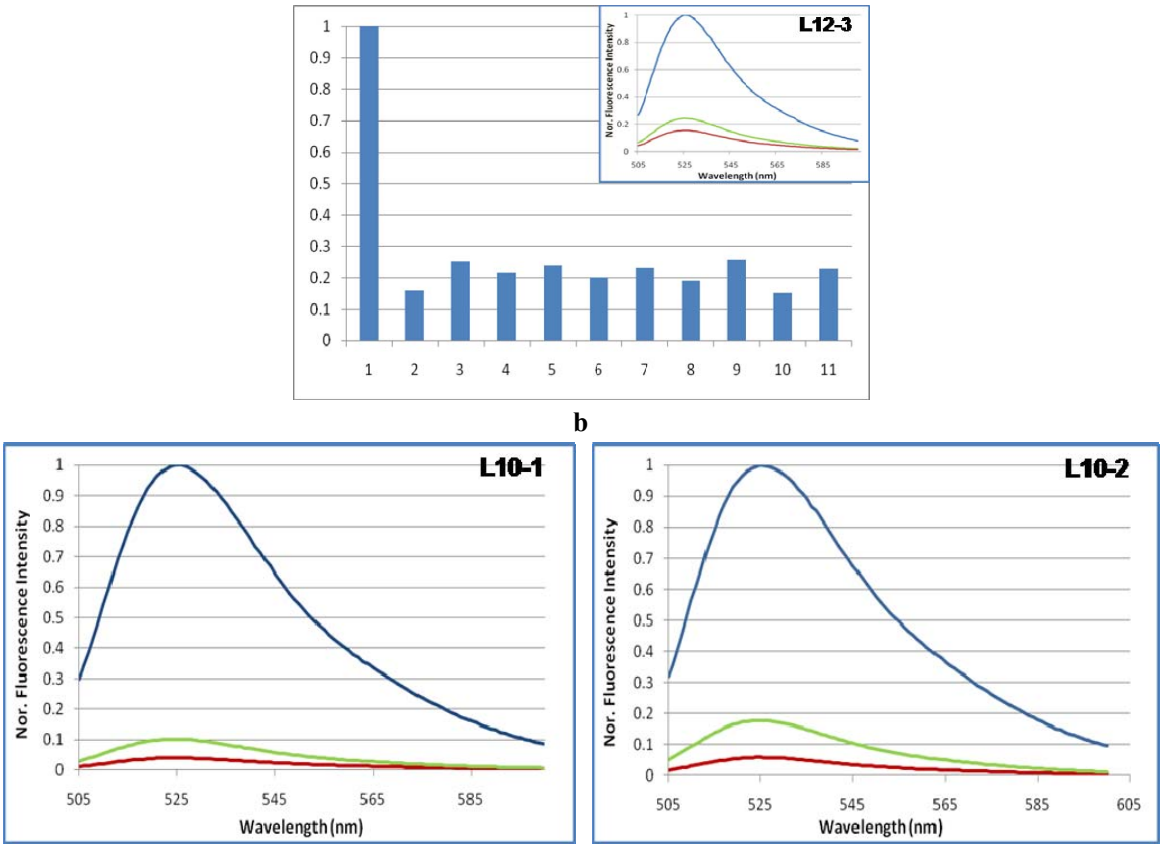

Figure S2. **a**) Fluorescence spectra of L12-1, L12-2 and L12-3(λ_{ex}= 488 nm) from top to bottom (left) after UV/Vis irradiations. All conditions are the same as PSMM1-3. **b)** Fluorescence spectra of L10-1 and L10-2. The brown curve is DNA in buffer solution after visible irradiation; blue line is with five times of cDNA; green line is after UV irradiation: Vis(450nm): 1 min; UV(350 nm): 10min (buffer: 20 mM Tris buffer pH 8.0, Na^+: 20 mM, Mg^{2+}: 2 mM). The figures on the right from top to bottom are the five cycles of UV/Vis irradiation.

We further synthesized and photoregulated ten-base linear DNAs (L10-1, L10-2) incorporated with three and four Azo-, respectively (**Table S1**). The T_ms of these two DNAs are nearly 8 degrees lower than PSMM3. We expected these linear DNAs to perform better under light cycling than L12 DNAs. Both L10-1 and L10-2 were photoregulated at the same conditions as PSMM3. The results displayed higher regulation efficiencies of 6.3% for L10-1 and 13.8% for L10-2 (**Figure S2b**). Although improvements in photo-responsiveness to UV/Vis irradiation are observed for these linear DNAs with shorter length and lower T_m, the efficiency of both L10-1 and L10-2 is still far below that of PSMM3. Taken together, these results indicate that the hairpin-based PSMMs are much more sensitive to photons than their linear DNA counterparts.

The specialized hairpin structure of PSMMs has been compared with another hairpin structure. While conventional DNA nanomotors involve only linear DNAs with single strand and duplex structures, PSMMs have a hairpin structure on the loop moiety that amplifies the impact of external stimuli (in this case, isomerization of azobenzene) on the open-close circulation, as determined by our experimentation. The hairpin structure can stabilize the stem duplex for comparable T_m with shorter base pairs than linear DNAs, with and without azobenzene moieties. To further examine the impact of the special hairpin structure on nanomotor efficiency, we designed a similar hairpin structure, PolyT(A3), for comparison. The PolyT(A3) has 31 bases with the same stem duplex as PSMM3, but only a T base on the loop moiety: **5' FAM-CCT AGC TTT TTT TTT TTT TTT TTT T-Azo-GC-Azo-TA-Azo-G G-**

Dabcyl 3' (underlined bases represent stem moieties). Three Azo- moieties were incorporated at the same positions as those in PSMM3. The photoregulation of this nanomotor also displayed high efficiency and photoreversibility (**Figure S3**). Moreover, the PolyT(A3) nanomotor had an average efficiency of 38.9% with at least five cycles of UV/Vis irradiation. As opposed to the structure of linear DNAs, these results illustrate that molecular motors based on hairpin structure do possess easier conversion structure for higher conversion efficiency. At the same time, their stability is not affected. The PolyT(A3), which has a T base loop, does have a tendency to form a more regular and symmetric structure, while PSMM3 molecules have specific loop structure by their asymmetric base sequences. Nevertheless, both the PolyT(A3)- and PSMM3-based nanomotors displayed high nanomotor efficiency, which gives conclusive evidence that the hairpin structure enables DNA nanomotors to gain highly efficient conversion.

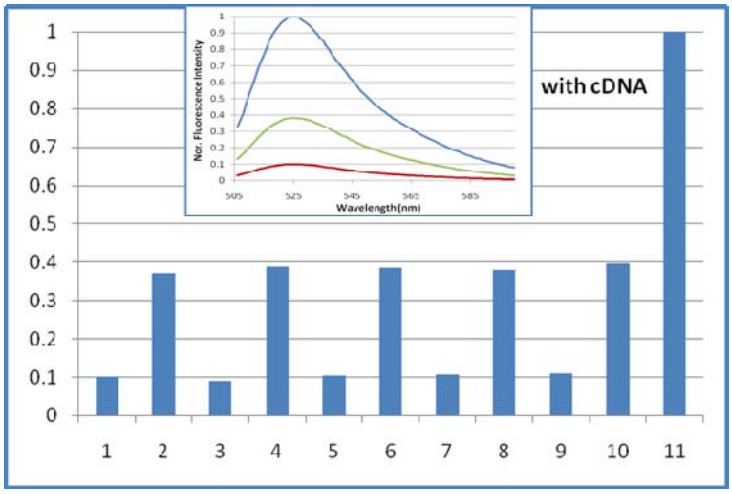

Figure S3. Fluorescence spectra of PolyT(A3) (λ_{ex}= 488 nm) under irradiation of 6W UV lamp (350 nm) and 60W desktop lamp with 450 nm filter at 25 $^{\circ}$C. The brown curve is the fluorescence intensity for pure DNA in buffer solution; blue line is the fluorescence intensity after five times of cDNA; green line is the fluorescence intensity after UV irradiation: Vis(450nm): 1min; UV(350nm): 5min. (buffer: 20mM Tris-HCl pH 8.0, 20mM Na^{+}: 2mM Mg^{2+}).

Table S1. **Comparison of all DNA sequences with and without Azo- incorporation**

Sequence Name	base number	Azo- number	Azo-/base ratio (%)	T_m (^{0}C) ±0.5^{0}C	Recovery (%)
MB	31	0	0	57.5	N/A
PSMM1	31	1	3.2	57.0	14.2 ±2.5
PSMM2	31	2	6.5	56.3	26.3 ±3.3
PSMM3	31	3	9.7	55.0	54.7 ±3.1
PolyT	31	3	9.7	54.9	31.3 ±2.5
L12-1	12	3	25	55.2	2.9 ±0.8
L12-2	12	4	33.3	54.8	5.7 ±1.1
L12-3	12	5	41.7	53.7	11.5 ±2.3
L10-1	10	3	30	47.5	6.3 ±1.6
L10-2	10	4	40	48.6	13.8 ±2.2

Table S2. **Conversion efficiency of PSMM3 and L10-1 in different concentrations**

Sequence Name	Conversion efficiency by recovery (%)			
	100 nM	500 nM	5 μM	50 μM
PSMM3	54.7 ±3.1	44.6 ±2.7	45.8 ±3.1	44.7 ±2.8
L10-1	6.3 ±1.3	9.0 ±1.2	4.4 ±0.6	0.7 ±0.2

Reference:

1. H. Asanuma, X. Liang, H. Nishioka, D. Matsunaga, M. Liu, M. Komiyama *Nature Protocols* **2007**, *2*, 203-213.
2. H.; Allawi, J. Jr. SantaLucia, *Biochemistry* **1997**, *36***,** 10581-10594.
3. B. Tinland, A. Pluen, J. Sturm, G. Weill, *Macromolecules* **1997**, *30*, 5763-5765.
4. Liang, X.; Nishioka, H.; Takenaka, N.; Asanuma, H. *ChemBioChem*, **2008**, *9*, 702–705.
5. Liang, X.; Asanuma, H.; Komiyama, M. *Tetrahedron Lett.* **2001**, 42, 6723–6725.
6. Asanuma, H.; Liang, X.; Yoshida, T.; Komiyama, M.*Chembiochem* **2001**, *2*, 39–44.
7. Liang, X.; Asanuma, H.; Komiyama, M. *J. Am. Chem. Soc.* **2002**, *124*, 1877–1883.
8. Asanuma, H.; Matsunaga, D.; Komiyama, M. *Nucleic Acids Symp. Ser.* **2005**, 49, 35–36.